A Practical Synthesis and X-Ray Crystal Structure of (E)-4-(1-naphthylvinyl)pyridine and Related Compounds

James G.D. Moffat, Victoria N.P. Pham-Tran, Katherine M. Marczenko*

Department of Chemistry, Carleton University, 1125 Colonel By Drive, Ottawa, Ontario, K1S 5B6, Canada.

Email: katherinemarczenko@cunet.carleton.ca.

Abstract

The synthesis, structure, and photoreactivity of (E)-4-(1-naphthylvinyl)pyridine ((E)-4-1-nvp; **1**) and its coordination compounds has been investigated. Synthesis of (**1**) via Wittig olefination resulted in a challenging isomer separation and purification process. By synthesizing (**1**) via a Horner-Wadsworth-Emmons reaction, high stereoselectivity and purity was achieved. The crystal structure of (**1**) revealed significant intramolecular rotation facilitated by CH···π interactions, ultimately preventing olefin stacking in both the solid-state structure of (**1**) and a cocrystal with a structural isomer. Novel Ag(I) and Zn(II) coordination complexes that utilize (**1**) as a ligand were also synthesized and fully characterized, facilitating the examination of the relationship between molecular planarity and secondary bonding contributions via Hirshfeld surface analyses. These findings deepen our understanding of intermolecular interactions involving (E)-4-1-nvp and offer insights for designing novel photoresponsive materials capable of solid-state [2+2] cycloaddition.

Key words: Horner Wadsworth Emmons, Wittig Olefination, X-Ray Crystallography, Photoresponsive Molecules.

Introduction

Light responsive materials are at the forefront of materials research due to their dynamic properties under light stimulus, making them valuable for applications in energy storage, biomaterials, sensing, and actuation.[1–3] Among these materials, arylvinylpyridine derivatives hold significant promise due to their ability to undergo photochemical isomerization and [2+2] cycloaddition in a controlled manner.[4–6] The versatility displayed by 4-styrylpyridine in light-responsive devices and materials with tunable properties further highlights the importance of this class of molecules. Recently, studies exploring the structural and photophysical properties of coordination polymers and metal-organic compounds incorporating (E)-4-(1-naphthylvinyl)pyridine ((E)-4-1-nvp; **Scheme 1a**) have emerged.[7–9] The metal-organic compounds $[Cd(quin)_2((E)\text{-}4\text{-}1\text{-}nvp)_2]$ (Hquin = quinoline-2-carboxylic) and $[Cd(4\text{-}1\text{-}nvp)_2(5\text{-}ssa)]\cdot((E)\text{-}4\text{-}1\text{-}nvp)$ (5-ssa = 5-sulfosalicylic acid) undergo thermally reversible topochemical [2 + 2] cycloaddition reactions under sunlight irradiation.[10,11] A Zn(II) based 1D coordination polymer, [Zn(cis-1,4-chdc)((E)-4-1-nvp)] (cis-1,4-H_2chdc = cis-1,4-cyclohexanedicarboxylic acid), exhibits solid-state photochemical [2 + 2] cycloaddition reactions under UV irradiation, resulting in mechanical motion such as swelling and bursting, whereas the Cd(II) counterpart undergoes photodimerization without such responses.[12] A more dramatic effect, the photosalient effect which is when crystals burst, pop, swell, and/or fragment, was observed when the 1D coordination polymer [Zn(glu)((E)-4-1-nvp)] (H_2glu = glutaric acid) was exposed to UV and sunlight irradiation.[13] A remarkable number of photosalient solids

utilize photochemical [2 + 2] cycloadditions of neighbouring (E)-4-1-nvp molecules, including a Zn(II) based 2D metal–organic framework, $[Zn_2(suc)_2((E)\text{-}4\text{-}1\text{-}nvp)_2]$ (H_2suc = succinic acid),[14] and the metal organic compound $[Zn(4\text{-}ohbz)_2((E)\text{-}4\text{-}1\text{-}nvp)_2]$ (H-4-ohbz = 4-hydroxy benzoic acid).[15]

Central to the architecture of these complexes is the extensive supramolecular network imposed by hydrogen bonding, CH···π, and π···π interactions through the incorporation of the (E)-4-1-nvp moiety.[16,17] These intermolecular interactions can assist with olefin stacking between neighboring molecules and increase the potential of photochemical transformations in the solid-state.[18] Despite the rapid evolution of (E)-4-1-nvp in the realm of photoresponsive material chemistry, a comprehensive understanding of its solid-state structure remains elusive. This gap highlights the need for further exploration into the intricate intermolecular forces dictating the behavior of (E)-4-1-nvp and its derivatives in the solid-state. Moreover, achieving precise control over the isomeric composition remains a significant challenge which must be overcome if we wish to optimize the photochemical behavior of such molecules and materials.

The Horner-Wadsworth-Emmons (HWE) reaction generally offers enhanced stereoselectivity for (E) alkene formation and produces a dialkylphosphate salt as a reaction by-product, which is easily removed by aqueous extraction.[19] This stands in contrast to the Wittig method, which is known for poor control of E/Z selectivity and the production of triphenylphosphine oxide, which is a challenging reaction by-product to remove using standard purification techniques.[20] Published synthetic routes for (E)-4-1-nvp predominantly utilize the Wittig reaction, overlooking these challenges.[21] Recent investigations, such as those by Nakamura *et al*. have underscored the advantages of

the HWE reaction for synthesizing similar photoresponsive molecules.[22] This reaction offers enhanced stereoselectivity and simplifies purification steps, both crucial for achieving the desired high isomeric purity of (**1**). Given these advantages over the Wittig approach, the HWE reaction stands out as a promising method for the synthesis of (E)-4-1-nvp and warrants further investigation.

Herein, a facile synthetic strategy for (**1**) is reported, utilizing the HWE reaction to produce a highly stereopure product with a minimal work-up procedure. The X-ray crystal structures and photochemical analyses of (E)-4-(1-naphthylvinyl)pyridine (**1**) and its derivatives bis[(E)-4-(1-naphthylvinyl)pyridine] zinc dichloride (**2**), a (E)-4-(1-naphthylvinyl)pyridine:(E)-2-(4-naphthylvinyl)pyridine co-crystal (**3**), and bis[(E)-4-(1-naphthylvinyl)pyridine] silver trifluoroacetate (**4**) are also obtained and photochemically assessed.

Experimental Details

General. Manipulations were performed either in air under standard atmospheric conditions or using standard Schlenk techniques under an atmosphere of dry nitrogen (see specific syntheses to determine which applies). Solvents were dried over Na/benzophenone (tetrahydrofuran, hexanes) and distilled prior to use. For air/moisture-free syntheses, reaction glassware was baking in a 140 °C oven for at least 2 hours prior to use and assembled under nitrogen while hot. All deuterated solvent was dried and stored over activated molecular sieves (3 Å). Triethyl phosphite (98%), 1-(chloromethyl)naphthalene (90%/97%), and n-butyllithium (1.6 M or 2.5 M in hexanes) were obtained from Sigma Aldrich. 4-pyridinecarboxaldehyde was obtained from Thermo Scientific.

All Nuclear Magnetic Resonance (NMR) experiments were carried out on a Bruker AV-300 spectrometer with residual solvent used for chemical shift calibration. Samples for NMR spectroscopy were prepared in dried deuterated solvent and spectra are referenced to tetramethylsilane (^{1}H). The NMR data were processed using Bruker TopSpin 4.3.0[23] and can be seen in **Figures S1-S9**.

Powder X-Ray Diffraction (PXRD) data (**Figures S10-S13**) were collected using a PANalytical Empyrean diffractometer in a reflection (Bragg-Brentano) geometry with Cu K_α radiation source, Ni K_β filter and PIXcel1D linear detector. Powder diffractograms were recorded in the 5-50° 2θ range with a step size of 0.01303°. Data collection was controlled with X'Pert Data Collector Software.[24]

Single-Crystal X-Ray Diffraction (SCXRD) experiments were run on a Rigaku MiniLab II diffractometer, equipped with a Mo source (λ = 0.71 Å) and Oxford 800 cryostream. Reflections were integrated using the CrysAlias Pro software (v43).[25] The structures were solved by intrinsic phasing and a full matrix least-squares refinement was carried out using all data in Olex2-1.5.[26] Non-hydrogen atoms were refined anisotropically, while hydrogen atoms were added in calculated positions. The crystallographic data for compounds (**1**)-(**4**) and (**4-THF**) are shown in **Table S1** and **S2**. CIFs have been deposited to the Cambridge Crystallographic Data Center with deposition numbers 2335560-2335564.

Solution UV-VIS spectra (**Figures S14-S17**) were obtained on a Shimadzu UV-2450 instrument using a high-performance single monochromator and an R-928 photomultiplier tube. Fluorescence spectra (**Figures S18-21**) were obtained on Shimadzu

RF-1501 spectrofluorophotometer using 150 W Xenon lamp with ozone resolving-type lamp housing. All samples were sandwiched between two (51 mm x 51 mm x 0.5 mm) glass slides. The infrared spectra of all solid compounds (**Figures S22-S25**) were obtained on an Agilent Cary 630 FTIR ZnSe engine instrument equipped with a single-bounce diamond ATR sampling accessory a standard globar source, and a DLaTGS detector. Differential Scanning Calorimetry (DSC) experiments (**Figures S26-S34**) were performed on a TA Instruments Q10 model. The DSC was calibrated at the melting point of the indium metal (156.6 °C). All DSC samples were hermetically sealed in aluminum pans prior to analysis. Melting points were measured as the peak temperature of an endothermic event.

Synthesis of Diethyl 1-Naphthylmethyl Phosphonate. A modified literature procedure was followed.[27] Triethyl phosphite (14.8 mL, 86.3 mmol) was added to 1-(chloromethyl)naphthalene (15.23 g, 86.22 mmol) under nitrogen and stirred vigorously for 20 minutes to produce a light yellow oil. The reaction was refluxed under nitrogen with an air-cooled condenser and stirred for 7 hours, turning the solution light amber in colour. (23.20 g, 98% yield). ^{1}H-NMR ($CDCl_3$, 300 MHz): 8.12 (1H, d, Ar-H), 7.85 (1H, d, Ar-H), 7.77 (1H, d, Ar-H), 7.48 (4H, m, Ar-H), 3.94 (4H, m, C-H), 3.64 (2H, d, C-H, J = 22 Hz), 1.15 (6H, t, C-H). ^{31}P-NMR ($CDCl_3$, 121 MHz): 28.72 ppm.

Synthesis of (E)-4-(1-naphthylvinyl)pyridine (1). To a solution of diethyl 1-naphthylmethyl phosphonate dissolved in 60 mL of anhydrous tetrahydrofuran (THF), 2.5 M of *n*-butyllithium (10.1 mL, 25.3 mmol) was added dropwise under nitrogen over a cold ice bath. The solution immediately turned bright orange, gradually becoming a dark and almost black colour. The reaction was then brought to room temperature with stirring for

2 hours. Pyridine-4-carboxaldehyde (2.4 mL, 25 mmol) was added dropwise, resulting in a light orange coloured solution, and left to stir overnight (~12 hours). 50 mL of a saturated ammonium chloride solution was added and subsequently extracted with dichloromethane (DCM; 3 x 20 mL). The organic phase was dried over magnesium sulphate, filtered, and condensed *in vacuo* to form a light orange oil. The oil was subsequently washed with hexane, solidifying into a light beige solid (5.2574 g, 90% yield). M.P = 75.6 °C ^{1}H-NMR ($CDCl_3$, 300 MHz): 8.63 (2H, d, Ar-H), 8.20 (1H, d, Ar-H), 8.12 (1H, d, *trans*-alkene, *J* = 16 Hz), 7.89 (2H, t, Ar-H), 7.78 (1H, d, Ar-H), 7.55 (3H, m, Ar-H), 7.48 (2H, d, Ar-H), 7.09 (1H, d, *trans*-alkene, *J* = 16 Hz) ppm. ^{13}C-NMR ($CDCl_3$, 75 MHz): 150.26, 144.86, 133.80. 133.74, 131.33, 130.90, 129.15, 129.03, 128.80, 126.53, 126.11, 125.66, 124.24, 123.47, 121.08 ppm.

Synthesis of bis[(E)-4-(1-naphthylvinyl)pyridine] zinc (II) dichloride, [Zn((E)-4-1-nvp)$_2$Cl$_2$] (2). A solution of (E)-4-1-nvp (0.1353 g, 0.585 mmol) in ethanol (EtOH; 2 mL) was prepared in a 4-dram vial, and a solution of $ZnCl_2(THF)_2$ (0.0830 g, 0.296 mmol) in EtOH (2 mL) was prepared in a separate 4-dram vial. Both solutions were heated to 35 ˚C and a stir bar was placed in the (E)-4-1-nvp solution vial. The $ZnCl_2(THF)_2$ solution was transferred to the (E)-4-1-nvp solution vial with stirring, resulting in the immediate precipitation of a light-yellow solid. This mixture was stirred for 3 hrs at room-temperature. The precipitate was collected using suction filtration, and washed with EtOH, deionized water, and diethyl ether, affording a light-yellow powder (0.1272 g, 67%). M.P = 243.7 °C ^{1}H-NMR ($CDCl_3$, 300 MHz) *∂*: 8.83 (4H, d, Ar-H), 8.25 (2H, d, *trans*-alkene, *J* = 16 Hz), 8.16 (2H, d, Ar-H), 7.91 (4H, d, Ar-H), 7.81 (2H, d, Ar-H), 7.71 (4H, d, Ar-H), 7.64-7.47 (6H, m, Ar-H), 7.13 (2H, d, *trans*-alkene, J = 16 Hz) ppm. ^{13}C-NMR (DMSO, 75 MHz):

149.92, 146.15, 133.84, 133.61, 131.32, 131.15, 129.57, 129.01, 128.85, 127.03, 126.61, 126.23, 124.46, 124.24, 122.26 ppm.

Synthesis of a (E)-4-(1-naphthylvinyl)pyridine:(E)-4-(2-naphthylvinyl)pyridine cocrystal (3). Crude (E)-4-1-nvp was diluted with methanol affording an insoluble white solid. The white solid was separated from the filtrate layer, yielding a (E)-4-1-nvp: (E)-4-1-nvp (1:1) co-crystal. M.P = 123.8 °C. ^{1}H-NMR ($CDCl_3$, 300 MHz): 8.62 (4H, m, Ar-H), 8.19 (1H, d, Ar-H), 8.12 (1H, d, *trans*-alkene, *J* = 16 Hz), 7.87 (6H, m, Ar-H), 7.77 (2H, t, Ar-H). 7.51 (10H, m), 7.15 (1H, d, *trans*-alkene, *J* = 16 Hz), 7.09 (1H, d, *trans*-alkene, *J* = 16 Hz) ppm. ^{13}C-NMR ($CDCl_3$, 75 MHz): 150.22, 150.12, 144.90, 144.80, 133.80, 133.74, 133.61, 133.55, 133.40, 131.33, 130.43, 129.16, 129.02, 128.80, 128.62, 128.24, 127.92, 127.79, 126.63, 126.60, 126.53, 126.21, 126.11, 125.66, 124.24, 123.46, 123.35, 121.07, 120.91 ppm.

Synthesis of bis[(E)-4-(1-naphthylvinyl)pyridine] silver (I) trifluoroacetate, [Ag((E)-4-1-nvp)$_2$O$_2$CCF$_3$] (4) and bis[(E)-4-(1-naphthylvinyl)pyridine] silver (I) trifluoroacetate bis(tetrahydrofuran), [Ag((E)-4-1-nvp)$_2$O$_2$CCF$_3$](C$_4$OH$_8$)$_2$ (4-THF). Silver trifluoroacetate (0.0284 g, 0.129 mmol) and (E)-4-1-nvp (0.0563 g, 0.243 mmol) were stirred together in 8 mL of THF with gentle heating until full dissolution. The solution was then stirred for 1 hour at room temperature. Single crystals were grown by solvent-solvent diffusion with approximately equal volumes of THF and diethyl ether to afford (**4-THF**). The procedure was repeated without heating in DCM to grow single crystals via slow evaporation, affording the THF-free form (**4**). (**4**): M.P = 180.6 °C. ^{1}H-NMR ($CDCl_3$, 300 MHz): 8.63 (4H, d, Ar-H), 8.26 (1H, s), 8.19 (3H, d), 7.91 (4H, m, Ar-H), 7.81 (2H, d, Ar-H), 7.64 (4H, d, Ar-H), 7.56 (6H, m), 7.16 (2H, d, *trans*-alkene, *J* = 16 Hz) ppm. ^{13}C-

NMR (DMSO, 75 MHz): 151.05, 145.65, 133.85, 133.67, 131.32, 130.86, 129.51, 129.02, 128.97, 127.02, 126.62, 126.24, 124.40, 124.25, 122.12 ppm.

Results and Discussion

Initial attempts to synthesize (E)-4-(1-naphthylvinyl)pyridine ((E)-4-1-nvp, **1**) followed literature procedure[8] and utilized a Wittig olefination (**Scheme 1-b-i**), wherein 1-(chloromethyl)naphthalene was refluxed with triphenylphosphine in toluene. This produced 1-naphthylmethylphosphonium chloride in high yield (90%). Subsequent deprotonation of the salt using aqueous sodium hydroxide (12% w/v) afforded a nucleophilic phosphorus ylide that, when reacted with pyridine-4-carboxaldehyde, gave a 70:30 mixture of (E):(Z) 4-1-nvp (**Scheme 1-b-ii**). Separation of triphenylphosphine oxide (TPPO) from the isomer mixture required at least 2-3 flash chromatography columns (90:10 EtOAc:diethyl ether). Furthermore, obtaining isomeric purity using flash chromatography was difficult and resulted in a dramatic reduction in yield. Attempts to crystallize TPPO from crude material using a benzene-cyclohexane solvent mixture resulted in a mixture of crystals of TPPO and (E)-4-1-nvp. Addition of zinc (II) chloride to an ethanol solution of crude material results in precipitation of $[Zn((E)\text{-}4\text{-}1\text{-}nvp)_2][Cl_2]$ (**2**), yielding mother liquor that contained only TPPO (**Scheme 1-b-iii**). Although this was selective at separating TPPO, coordinated ligand (**1**) was not labile enough to remove from the zinc complex, rendering this separation method unsuccessful.

Difficulties with the removal of TPPO, coupled with a lengthy isomer separation procedure prompted a reassessment of our synthetic strategy. Using the Horner-Wadsworth-Emmons (HWE) reaction offered distinct advantages over Wittig, providing a more stereoselective product yield and more easily removed reaction by-products.

Synthesis of the HWE phosphonate precursor followed a modified literature procedure,[27] wherein 1-(chloromethyl)naphthalene was refluxed in a stoichiometric amount of triethyl phosphite (**Scheme 1-b-iv**). This gave diethyl 1-naphthylmethyl phosphonate in excellent yield (96%) and did not require further purification before proceeding to the next synthetic step. Deprotonation of the phosphonate was achieved using *n*-butyl lithium (1.6 M in Hexanes) at 0 ˚C in THF, affording a phosphonate stabilized carbanion that was subsequently reacted with pyridine-4-carboxaldehyde, producing a 95:5 (E):(Z) product mixture of 4-1-nvp (**Scheme 1-b-v**) as determined by NMR spectroscopy. Tewari *et. al.* demonstrated that the reaction of dimethyl benzylphosphonate carbanions with aromatic aldehydes yields only the *trans* diaryl product.[28] To the best of our knowledge, this reactivity had not been extended to a naphthylphosphonate carbanion until now.

Both the Wittig and HWE syntheses require the precursor 1-(chloromethyl)naphthalene. This reagent is readily available as a liquid of 90% purity, and less commonly as a technical grade reagent of 97% purity. The supplier Sigma Aldrich notes that 2-(chloromethyl)naphthalene is the 10% impurity in the 90% grade. Although evidence of Wittig olefin of 2-(chloromethyl)naphthalene is never observed, we presume that a small amount of (E)-4-(2-naphthylvinyl)pyridine ((E)-4-2-nvp) was synthesized and removed during column chromatography. Purification of crude product resulting from HWE synthesis through sequential recrystallizations from methanol results in the formation of a 1:1 cocrystal of (E)-4-1-nvp:(E)-4-2-nvp (**3**) (**Scheme 1-b-vi**). Dissolution of this solid in acetonitrile resulted in selective precipitation of (E)-4-2-nvp. We have not observed evidence of the (E)-4-2-nvp byproduct since our exclusive use of the 97% reagent following the discovery of the cocrystal.

With a facile synthetic route towards (**1**) established, we then sought to test its stability and photoreactivity in solution and solid phases. The UV-Vis spectrum (**Figure S14**) of a chloroform solution of (**1**) shows a strong absorbance at 328 nm (π–π^* electronic transition) corresponding to *trans* to *cis* isomerization. Solutions of (**1**) are stable indefinitely in the dark, but slowly convert to (Z)-4-1-nvp when left in ambient light. This conversion is promoted via exposure to UV light (λ = 395 nm) and can be tracked using ^{1}H NMR spectroscopy (**Figure S3**). Concentrated neutral solutions of (**1**) do not show any evidence of photochemical [2 + 2] cycloaddition. This finding aligns with the observations made by Yamada and Nojiri, who showed that HCl is required for the promotion of photochemical [2 + 2] cycloaddition of (**1**) in solution by the preorientation of substrates through cation-π interactions.[29]

Crystals of (**1**) are readily grown via slow evaporation of DCM solutions at room temperature, or from a methanol solution at –30 °C. Solid-state photoluminescence measurements of these crystals show an emission maximum at 435 nm (**Figure S18**). No macroscopic physical changes to the crystals were observed when they were exposed to UV light (λ = 365 & 395 nm) for extended periods of time. NMR spectroscopy confirmed that (**1**) did not undergo chemical changes in the solid-state, which we hypothesize stems from the failure to meet the criteria outlined by Schmidt[30] for photochemical [2 + 2] cycloaddition. Schmidt noted two essential criteria for dimerization to occur: the double bonds of crystalline reactants must be parallel to each other, and the center-to-center distance of the reacting olefins must be less than 4.2 Å apart. When these criteria are satisfied, photochemical cycloaddition was predicted to proceed under topochemical control, selectively producing the regio- and stereoisomer dictated by the molecular

packing of the alkenes in the crystal. Indeed, the crystal structure of (**1**) revealed that Schmidt's criteria are not met.

Compound (**1**) crystallizes in the $P\bar{1}$ space group where Z' = 4 (**Figure 1a**) and Z = 8. No significant differences exist in the orientation of the four independent molecules and all bond angles and lengths are within three standard deviations of one another. Unit cell parameters were obtained at both ambient (293 K) and low temperatures (115 K) to confirm the absence of a temperature induced phase transition. All four independent molecules are non-planar, with intramolecular torsion angles spanning 48-51°. The intramolecular torsion angles are defined as the angle between the planes comprised of the pyridine and naphthalene rings. This torsion creates a "herringbone-like" packing structure when viewing down the *a*-axis, which is stabilized by CH···N and CH···π intermolecular interactions. However, only CH···π intermolecular interactions exist between the four independent molecules in the asymmetric unit. Molecular dynamic calculations on 4-styrylpyridine have shown that the molecular structure is strictly planar at the minimum associated with the *trans* isomer.[31] The structure becomes markedly twisted at the peak of the energetic barrier (transition state) associated with isomerization to the *cis* isomer. Hybrid density functional theory similarly predicts a planar ground state for (**1**) (**Figure S35**). From this, we can deduce that CH···π interactions play an important role in stabilizing the energetically less favorable non-planar geometry in the crystal structure.[32] Unfortunately, this torsion is an impediment for the parallel alignment of olefin moieties, which explains the lack of solid-state photochemical [2 + 2] cycloaddition.

Similarly, molecules of the (E)-4-1-nvp isomer in the crystal structure of (**3**) also deviate from planarity, albeit to a lesser extent (25°). SCXRD was used to confirm the

identity of a 1:1 (E)-4-1-nvp: (E)-4-2-nvp cocrystal. Compound (**3**) crystallizes in the $P2_1/n$ space group with Z' = 1 and Z = 4. The asymmetric unit contains one molecule of (E)-4-1-nvp and one molecule of (E)-4-2-nvp. The structure contains independent layers of (E)-4-1-nvp and (E)-4-2-nvp molecules rotated ~70° from each other and arranged along the *bc* plane. The primary intermolecular interaction within these layers are CH···N interactions between molecules of the same isomer (1': 2.744(2), 2': 2.563(2) Å). Intermolecular CH···N interactions do not exist between molecules of the different isomers. Instead, CH···π interactions are responsible for association of these molecular isomers in the solid-state. Although intramolecular torsion is observed in the geometry of the (E)-4-1-nvp isomer, the (E)-4-2-nvp isomer is completely planar. Because the structure contains alternating layers of (E)-4-1-nvp and (E)-4-2-nvp, intramolecular torsion of (E)-4-1-nvp prevents olefin alignment and adherence to Schmidt's criteria[30] for solid-state photochemical [2 + 2] cycloaddition. Crystals of (**3**) produced a red-shifted emission spectrum when compared to that of (**1**), with an emission maximum of 485 nm (**Figure S20**). DSC was used to confirm the formation of cocrystal (**3**), rather than a superposition of crystals of the individual isomers. The DSC thermogram for (**3**) shows an endothermic peak having an onset point of 120.7 °C and an enthalpy of fusion of 102.7 J/g. The DSC thermogram of (**1**) shows an endothermic peak having an onset temperature of 72.3 °C and an enthalpy of fusion of 63.6 J/g. No exothermic peaks were observed for (**1**) upon cooling. However, cycling of (**3**) did yield a distinct exothermic event with an onset temperature of 82.5 °C and an enthalpy of crystallization of 47.2 J/g. A significant shift in the onset of endothermic events from (**1**) to (**3**) and the formation of

new exothermic peaks in the DSC data of (**3**) supports crystallographic evidence for the formation of a cocrystal.

Although compound (**2**) was isolated through the unsuccessful purification of (**1**), we sought to establish its structure and propensity for photochemical [2 + 2] cycloaddition in the solid-state, as numerous photoresponsive materials are comprised of coordination compounds regulated by the participating metal ions. SCXRD revealed that (**2**) crystallizes in the *C*2/*c* space group with Z' = 0.5 and Z = 4. The molecular structure contains one zinc atom in a tetrahedral geometry (∠Cl–Zn–N 108.9(1)°) with a *cis* arrangement of chloro and (E)-4-1-nvp ligands. The bond lengths and angles of the (E)-4-1-nvp ligand are within agreement of what is observed in the structure of (**1**), and the Zn–N (2.061(1) Å) and Zn–Cl (2.211(1) Å) bond lengths agree with what is observed for a Zn(II) center. Unlike the structures of (**1**) and (**3**), the (E)-4-1-nvp ligand in (**2**) is completely planar. We turned towards Hirshfeld surface analysis to understand how this impacts the contribution of various intermolecular contacts to the Hirshfeld surface (**Table S3**). The two-dimensional fingerprint plot (**Figure S36**) revealed the highest percentage of C···C interactions out of all molecules presented in this study (**1**: 2.5%, **2**: 9.3%, **3**: 0.6%, **4**: 6.2%). This can be rationalized by examining the packing structure of (**2**). Chains run along the *a*-axis, yielding a herringbone packing structure facilitated by CH···π intermolecular interactions. Intermolecular π···π interactions occur between stacks of molecules running along the *b*-axis, specifically between the pyridine portion of one molecule and the naphthalene ring of another. However, this "head-to-tail" type arrangement results in displacement of the olefin moieties by one entire length of *b* and is facilitate by intermolecular π···π interactions. Exposure of crystals to UV light resulted

in no macroscopic physical or chemical change, indicating a lack of solid-state photochemical [2 + 2] cycloaddition. Ultimately, the analysis of the crystallographic data is consistent with Schmidt's criteria for photoreactivity, as the olefins are beyond the 4.2 Å distance required, despite the planarity of the molecular conformation.

Lastly, we attempted to use argentophilic forces, in the form of Ag···Ag interactions, to promote photochemical [2 + 2] cycloaddition through the formation of an Ag(I) coordination complex. This was inspired by the work of MacGillivray and others, the former of whom showed that templating (E)-4-styrylpyridine – the benzyl analogue of (**1**) – with Ag(I) ions resulted in intermolecular photochemical [2+2] cycloaddition.[33–35] Moreover, *intra*molecular photochemical [2 + 2] cycloaddition was achieved through the use of both a templating Ag(I) ion and a tethered analogue of (**1**); 1,8-bis[(E)-2-(4-pyridyl)ethenyl] naphthalene.[18] Stirring a solution of 2 equivalents of (E)-4-1-nvp with one equivalent of silver trifluoroacetate in THF for one hour at room temperature, and subsequent layering with diethyl ether, resulted in the formation of crystals of $[Ag((E)\text{-}4\text{-}1\text{-}nvp)_2(O_2CCF_3)_2](THF)_2$ (**4-THF**). Repeating the synthesis in DCM yields crystals of a THF free form (**4**) after three days of slow evaporation at room temperature (**Scheme 1-c**).

Compound (**4**) crystallizes in the $P\bar{1}$ space group whereas (**4-THF**) crystallizes in the $P2_1/c$ space group. The asymmetric unit of both structures contain one Ag atom coordinated to two molecules of (E)-4-1-nvp and one trifluoroacetate anion. The fluorine atoms of the anion exhibit rotational disorder. The structure of (**4-THF**) also contains two molecules of THF in the asymmetric unit which are disordered across a special position (see SI for more details). The Ag–N bonds are slightly elongated in (**4**) (**4**: 2.179(2),

2.172(2); **4-THF**: 2.165(2), 2.168(2) Å) whereas the N–Ag–N angles are identical and deviate slightly from linearity (**4**: 168.96(8)°; **4-THF**:168.40(7)°). The structure of (**4**) and (**4-THF**) each contain one planar and one twisted (E)-4-1-nvp ligand (**4**: 48.1°, **4-THF**: 44.2°). This intramolecular rotation is once again facilitated by CH···π interactions. Even with this rotation, the intermolecular Ag···Ag distances (**4**: 3.2470(4); **4-THF** 3.3097(3 Å) are shorter than what was reported by MacGillivray in the benzyl (3.4369(5) Å)[33] and tethered (3.3950(4) Å)[18] analogues. Although there is intermolecular alignment between the olefin pairs, the distances (**4**: 4.437(1), **4-THF**: 4.674(1) Å) exceed that defined by Schmidt's criteria (4.2 Å)[30], and crystals of both (**4**) and (**4-THF**) are photo-inert.

In conclusion, the synthesis of (E)-4-1-nvp (**1**) was initially explored through Wittig olefination, leading to challenges in isomer separation and yield reduction due to the production of triphenylphosphine oxide. This prompted a shift to the Horner-Wadsworth-Emmons reaction, offering improved stereoselectivity and easier removal of by-products. This synthetic refinement was complemented by an investigation into the stability and photoreactivity of (**1**) in solution and solid phases. While solution-phase UV-Vis and NMR studies revealed light-induced isomerization, solid-state studies elucidated the structural intricacies governing the lack of solid-state [2 + 2] cycloaddition. Notably, crystallographic analyses revealed the non-planarity of (**1**), driven by stabilizing CH···π interactions. Although the zinc coordination compound (**2**) resulted from an unsuccessful purification attempt of (**1**), crystallographic analysis revealed a planar (E)-4-1-nvp ligand. Ultimately, intermolecular π···π interactions displaced the olefin moieties beyond the distance required for solid-state [2+2] cycloaddition. Compound (**3**) represented a cocrystal of (E)-4-1-nvp and (E)-4-2-nvp. While the (E)-4-2-nvp isomer exhibited complete planarity, the

(E)-4-1-nvp isomer displayed intramolecular torsion, preventing alignment of the olefin moieties necessary for solid-state [2+2] cycloaddition.

Lastly, attempts to induce solid-state [2 + 2] cycloaddition through templating with argentophilic forces yielded structurally characterized compounds (**4**) and (**4-THF**). Both contain intermolecular olefin distances beyond those requisite for cycloaddition due to the presence of intramolecular torsion of one of the ligands, facilitated by stabilizing CH···π interactions. Overall, these findings contribute to a deeper understanding of the structural factors influencing the photoreactivity of (E)-4-1-nvp and its derivatives and pave the way for future design strategies in photoresponsive materials.

Acknowledgements

We acknowledge Carleton University for research funding in the form of start-up funds and a research development grant. We appreciate assistance from Kyle Fournier in the Chemical Instrumention Laboratory at Carleton University.

Author Contributions

J.M. synthesized (E)-4-1-nvp following Wittig and HWE procedures and isolated compounds (**2**) and (**3**). V.P.T synthesized compounds (**4**) and (**4-THF**). Characterization was split between J.M. and V.P.T. K.M.M. completed the crystallography. All authors contributed to the final version of the manuscript. K.M.M. conceived and supervised the project.

Figures and Figure Captions

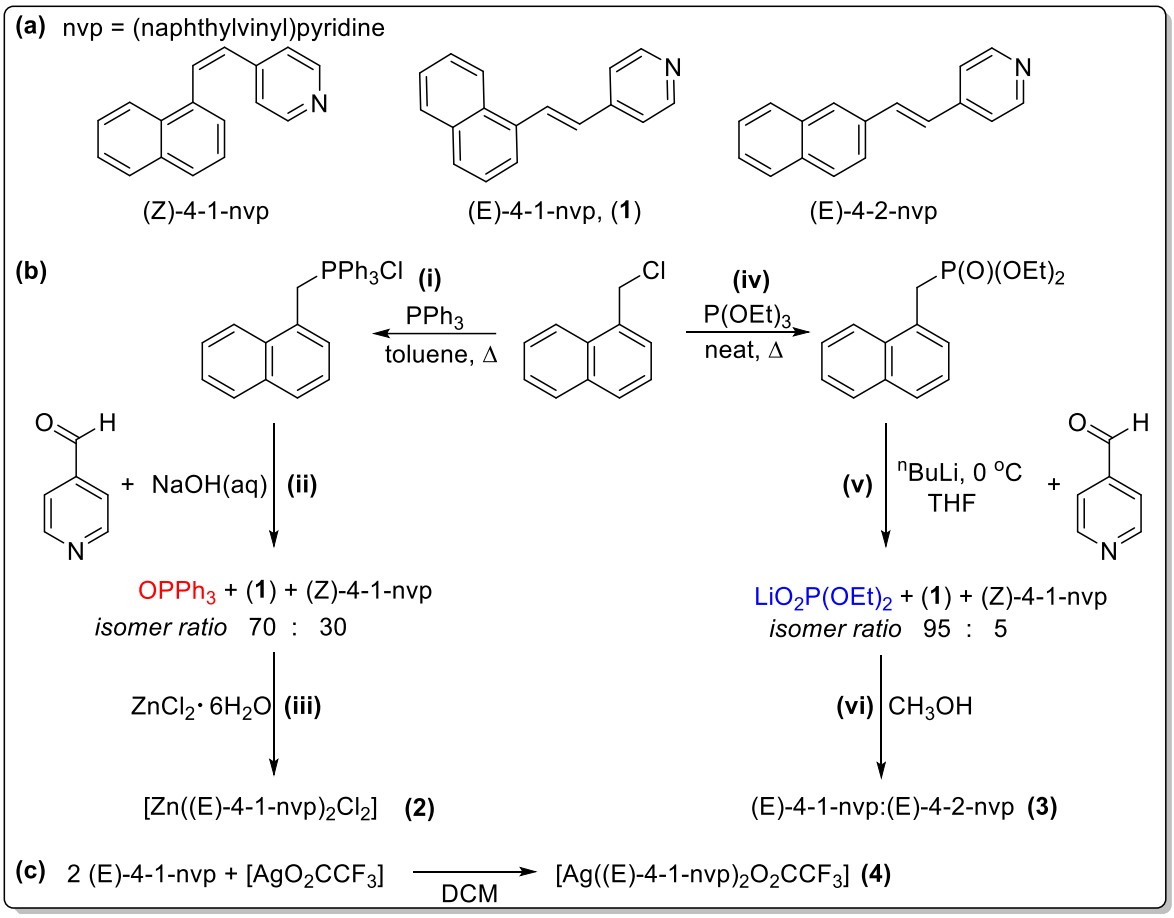

Scheme 1. a) The molecular structures of (Z)-4-(1-naphthylvinyl)pyridine (abbreviated (Z)-4-1-nvp), (E)-4-(1-naphthylvinyl)pyridine (abbreviated (E)-4-1-nvp, (**1**)), and (E)-4-(2-naphthylvinyl)pyridine (abbreviated (E)-4-2-nvp). **b**) The synthesis of (**1**) via Wittig olefination (i, ii) and Horner Wadsworth Emmons modification (v, vi), and the isolation of compounds (**2**; iii) and (**3**; vi). **c**) Synthesis of the silver complex (**4**).

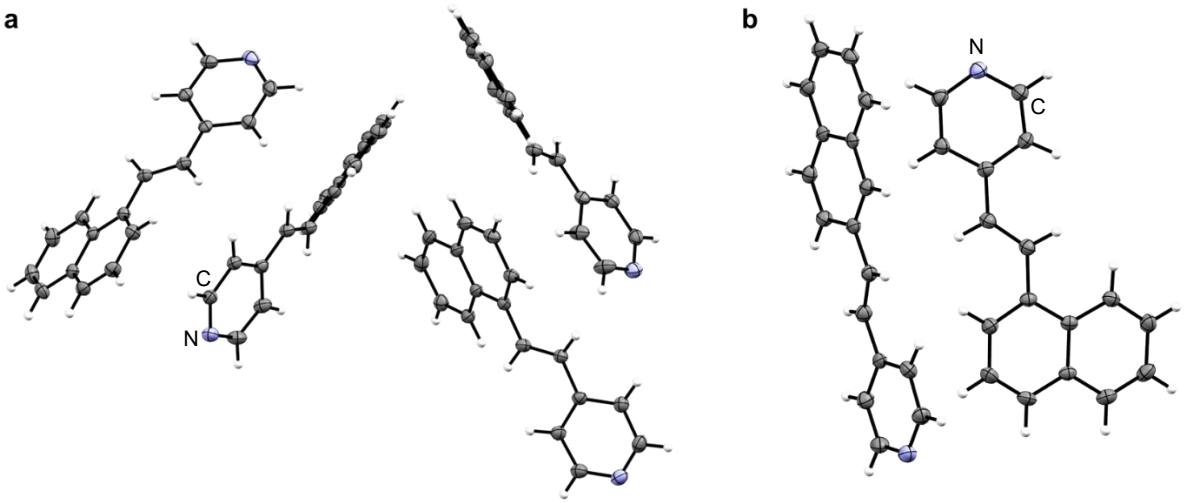

Figure 1. Single crystal x-ray structure of (**a**) compound (**1**) and (**b**) compound (**3**). The asymmetric units are shown and thermal ellipsoids are drawn at the 50% probability level.

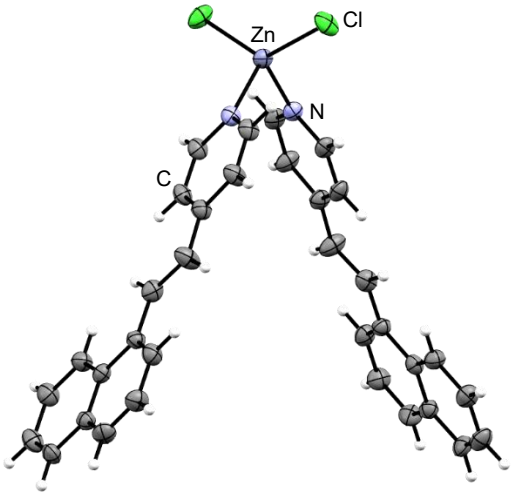

Figure 2. Single crystal x-ray structure of compound (**2**). Thermal ellipsoids are shown at the 50% probability level.

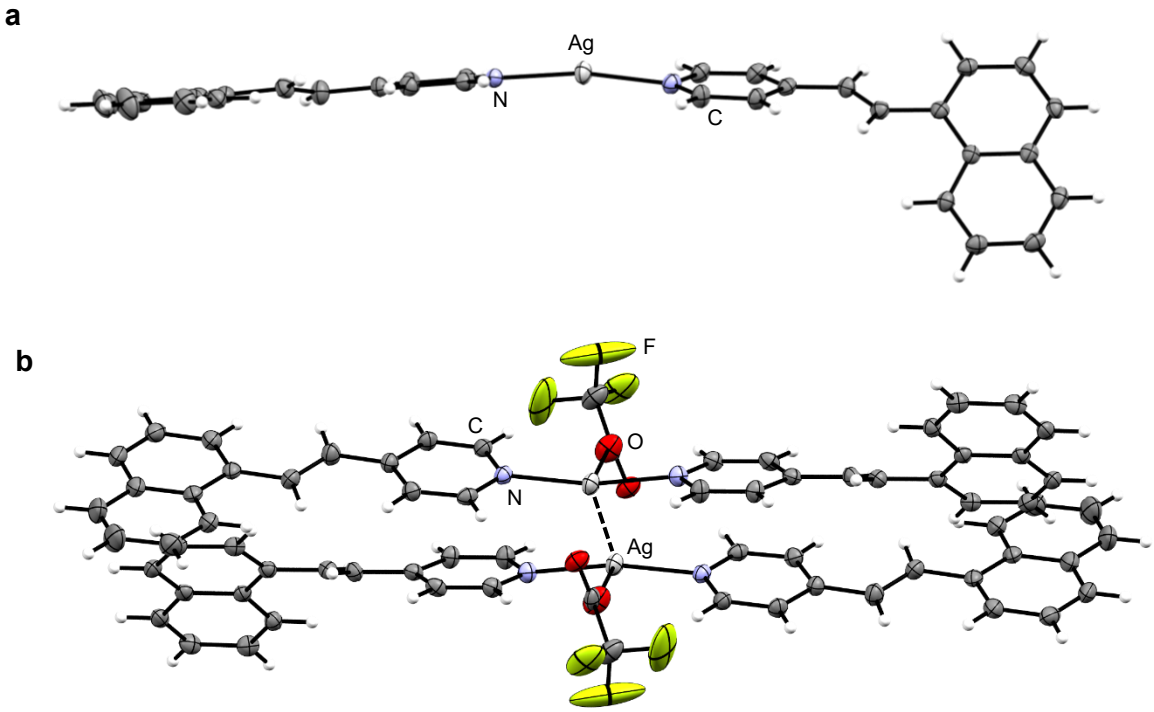

Figure 3. Single crystal x-ray structure of compound (**4**) showing (**a**) the planar geometry and intramolecular rotation of the (E)-4-1-nvp ligands and (**b**) the Ag···Ag intermolecular interaction and stacking of the olefin moieties. Thermal ellipsoids are shown at the 50% probability level and the [$O_2C_2F_3$] anion was omitted from (**a**).

References

1. Naumov, P., Chizhik, S., Panda, M. K., Nath, N. K., Boldyreva, E. *Chem. Rev.* **2015**, *115*, 12440–12490.
2. Goulet-Hanssens, A., Eisenreich, F., & Hecht, S. Adv. Mat. **2020**, *32*, 1905966.
3. Clerc, M., Sandlass, S., Rifaie-Graham, O., Peterson, J. A., Bruns, N., de Alaniz, J. R., Boesel, L. F. *Chem. Soc. Rev.* **2023**, *52*, 8245–8294
4. Friščić, T., MacGillivray, L. R. *Z. fur Krist. - Cryst. Mater*. **2005**, *220*, 351–363.
5. MacGillivray, L. R., Papaefstathiou, G. S., Friščić, T., Hamilton, T. D., Bučar, D. K., Chu, Q., Varshney, D. B., Georgiev, I. G. *Acc. Chem. Res*. **2008**, *41*, 280–291.
6. Ramamurthy, V., Sivaguru, J. *Chem. Rev.* **2016**, *116*, 9914–9993.
7. Dutta, B., Jana, R., Sinha, C., Ray, P. P., Mir, M. H. *Inorg. Chem. Front.* **2018**, *5*, 1998–2005.
8. Dutta, B., Dey, A., Sinha, C., Ray, P. P., Mir, M. H. *Inorg. Chem.* **2018**, *57*, 8029–8032.
9. Dutta, B., Hazra, A., Dey, A., Sinha, C., Ray, P. P., Banerjee, P., Mir, M. H. *Cryst. Growth Des.* **2020**, *20*, 765–776.
10. Mir, M. H., Bera, S., Khan, S., Maity, S., Sinha, C., Dutta, B. *Chem. Commun.* **2021**, *57*, 6197–6200.
11. Dutta, B., Dey, A., Sinha, C., Ray, P. P., Mir, M. H. *Inorg. Chem.* **2019**, *58*, 5419–5422.
12. Khan, S., Naaz, S., Ekka, A., Dutta, B., Roy, S., Medishetty, R., Mir, M. H. *Chem. Commun.* **2022**, *58*, 12102–12105.
13. Dutta, B., Sinha, C., Mir, M. H. *Chem. Commun.* **2019**, *55*, 11049–11051.

14. Bera, S., Dutta, B., Mandal, D., Sinha, C., Mir, M. H. *Inorg. Chem.* **2022**, *61*, 13244–13249.

15. Khan, S., Dutta, B., Naaz, S., Choudhury, A., Cazade, P. A., Kiely, E., Guerin, S. Medishetty, R., Mir, M. H. *Commun. Chem.* **2023**, *6*, 150.

16. Dutta, B., Dey, A., Maity, S., Sinha, C., Ray, P. P., Mir, M. H. *ACS Omega*, **2018**, *3*, 12060–12067.

17. Dutta, B., Hazra, A., Datta, S., Sinha, C., Banerjee, P., Mir, M. H. *ACS Appl. Polym. Mater.* **2022**, *4*, 2841–2850.

18. Laird, R. C., Sinnwell, M. A., Nguyen, N. P., Swenson, D. C., Mariappan, S. S., MacGillivray, L. R. *Org. Lett.* **2015**, *17*, 3233–3235.

19. Boutagy, J., Thomas, R. *Chem. Rev. 74*, 87–99.

20. Batesky, D. C., Goldfogel, M. J., Weix, D. J. *J. Org. Chem*. **2017**, *82*, 9931–9936.

21. Hu, F. L., Wang, S. L., Abrahams, B. F., Lang, J. P. *CrystEngComm*. **2015**, *17*, 4903-4911.

22. Nakamura, A., Irie, H., Hara, S., Sugawara, M., & Yamada, S. *Photochem. Photobiol.Sci.* **2011**, *10*, 1496–1500.

23. Bruker Biospin. TopSpin Software Version 4.0.7. **2017**, Karlsruhe, Germany: Bruker Biospin GmbH.

24. PANalytical. X'Pert Data Collector Software (Version 5.3.0.62) **2015**, Almelo, Netherlands: PANalytical B.V.

25. Agilent. CrysAlis PRO. **2014**, Agilent Technologies Ltd, Yarnton, Oxfordshire, England.

26. Dolomanov, O. V., Bourhis, L. J., Gildea, R. J., Howard, J. A. K., & Puschmann, H. *J. Appl. Crystallogr.* **2009**, *42*, 339–341.

27. Carrera, M., de la Viuda, M., & Guijarro, A. *Synlett*, **2016**, *27*, 2783–2787.

28. Tewari, R. S., Kumari, N., & Kendurkar, P. S. *J. Chem. Eng. Data*, **1976**, *21*, 125–131.

29. Yamada, S., & Nojiri, Y. *Molecules*, **2017**, *22*, 491.

30. Schmidt, G. M. J. *Pure Appl. Chem*. **1971**, *27*, 647–678.

31. Lawson Daku, L. M., Linares, J., & Boillot, M. L. *ChemPhysChem*, **2007**, 8, 1402–1416.

32. Nishio, M. *CrystEngComm*, **2004**, *6*, 130–158.

33. Chu, Q., Swenson, D. C., & MacGillivray, L. R. *Angew. Chem. Int. Ed.* **2005**, *44*, 3569–3572.

34. Blake, A. J., Champness, N. R., Chung, S. S., Li, W. S., Schröder, M. *Chem. Commun*. **1997**, *17*, 1675–1676.

35. Jung, O. S., Kim, Y. J., Lee, Y. A., Kang, S. W., & Choi, S. N. *Cryst. Growth Des*. **2004**, *4*, 23–24.